α decay chains from $Z = 118$ superheavy nuclei in the range $271 \leqslant A \leqslant 310$

K. P. Santhosh* and B. Priyanka

School of Pure and Applied Physics, Kannur University, Swami Anandatheertha Campus, Payyanur 670327, Kerala, India

(Received 10 April 2014; revised manuscript received 19 May 2014; published 11 June 2014)

An extensive investigation on the α decay properties of the isotopes of the superheavy nuclei with $Z = 118$, within the range $271 \leqslant A \leqslant 310$, has been performed within the Coulomb and proximity potential model for deformed nuclei. The α decay half-lives of $^{294}118$ and its decay products, evaluated using our formalisms, are in good agreement with the experimental results. The calculated α half-lives were also found to be matching well with the values computed using the Viola-Seaborg systematic, the universal curve of Poenaru *et al.* [Phys. Rev. C **83**, 014601 (2011); **85**, 034615 (2012)] and the analytical formulas of Royer [J. Phys. G: Nucl. Part. Phys. **26**, 1149 (2000)]. So as to identify the mode of decay of these isotopes, the spontaneous-fission half-lives were also evaluated for all the isotopes under study and, our prediction of 3α chains from $^{294}118$ go hand in hand with the experimental observations. Our study also unveils that those isotopes of $Z = 118$ with $A \geq 301$ and with $A \leqslant 275$ do not survive fission, thus restricting the α decay within the range of $276 \leqslant A \leqslant 300$, and we hope that the theoretical prediction of 5α decay chains consistently from $^{289-293}118$ isotopes provides a new perspective to experimentalists.

DOI: 10.1103/PhysRevC.89.064604 PACS number(s): 23.60.+e, 23.70.+j, 25.85.Ca, 27.90.+b

I. INTRODUCTION

The past few decades have witnessed tremendous strides in the production and spectroscopic studies of heavy elements owing to the prodigious advancements in the heavy-ion beam technologies and accelerator facilities. The synthesis and identification of new isotopes in the superheavy region is one of the most rewarding and challenging investigations for the experimental nuclear physicists and these new discoveries are aimed at expanding, simultaneously, the periodic table of elements and the Segre chart of nuclei [1]. Recent experiments and those in progress at various laboratories drive at validating the predictions made within several theoretical approaches and hypotheses that can be traced back to 40 y on the existence of an enhanced stability in the region of the superheavy nuclei (SHN) [2]. The prediction of the existence of a "magic island" or the "island of stability," around $Z = 120$, 124, or 126 and $N = 184$ [3], in the domain of the superheavy elements may be quoted as one of the fundamental outcomes of the nuclear shell model. The heaviest neutron-rich nuclei with $N > 170$ in the vicinity of the closed spherical shells, $Z = 114$ (or possibly 120, 122, or 126) and $N = 184$, were expected to mark a considerable increase in nuclear stability, similar to the effect of the closed shells on the stability of doubly magic ^{208}Pb ($Z = 82$ and $N = 126$) [4]. Hence, several experiments were performed by Oganessian *et al.* [1,2,4–7] with the purpose of synthesizing SHN close to the predicted neutron magic number $N = 184$, through the complete fusion reactions of long-lived even-Z target nuclei ^{242,244}Pu, ^{249}Cf, and ^{248}Cm with ^{48}Ca projectiles with the maximum accessible neutron richness.

In reviewing the production of a century of radioactive elements up to $Z = 119$ [8–10], historically [11,12], different periods have to be considered, both theoretically and experimentally. The development of the particle accelerators and particle detectors during the mid-20th century [13] brought about the techniques of fusing light elements with long-lived isotopes of the heaviest actinides (^{233,238}U, ^{237}Np, ^{242,244}Pu, ^{243}Am, ^{245,248}Cm, and ^{249}Cf) produced in nuclear reactors, usually termed as the "hot fusion" or "actinide-based fusion" as the compound nuclei formed after fusion is hot owing to excitation energies between 40 and 50 MeV. SHN with $Z =$ 113–116 [4–6] and 118 [1,2] have been synthesized at Joint Institute for Nuclear Research-Flerov Laboratory of Nuclear Reactions (JINR-FLNR), Dubna, in collaboration with the Lawrence Livermore National Laboratory researchers using this method and very recently the authors were also successful in the synthesis of two isotopes of $Z = 117$ [14,15]. Later, the 1970s [16,17] witnessed the synthesis of heavier elements through the fusion of the closed-shell nuclei ^{208}Pb and ^{209}Bi, with the medium-mass neutron-rich isotopes such as ^{54}Cr to ^{70}Zn. The SHN with $Z = 107$ to 112 were synthesized at GSI, Darmstadt [8,18–21] using this method and an isotope of $Z =$ 113 has been identified at Rikagaku Kenkyusho (RIKEN), Japan [22,23], and they have also reconfirmed [24,25] the existence of the superheavy elements $Z = 110$, 111, and 112 reported earlier by GSI group. This method employed for the production of SHN at excitation energies of 10–20 MeV, whereby the compound systems stay colder than in hot-fusion reactions, was called "cold fusion"/"cluster-based fusion" or the neutral "Pb/Bi-based fusion."

Even though, the choice of the target and projectile combination for the synthesis of SHN is posed as the common limitation in the hot-fusion reactions and cold-fusion reactions, the doubly magic ^{48}Ca, similar to ^{208}Pb, was proposed [10,23] as the projectile for both these reactions. The synthesis of many superheavy elements with $Z < 119$, during past three decades is mainly based on this idea [7,8] and Oganessian *et al.* [6] have reported the synthesis of $^{294}118$ as the product of the $3n$-evaporation channel of the ^{249}Cf (^{48}Ca, xn)$^{297-x}118$ reaction, and recently they have been successful in synthesizing $^{294}118$ via the fusion of ^{249}Cf and ^{48}Ca [1,2].

*drkpsanthosh@gmail.com

TABLE I. The α decay half-lives of $^{294}118$ and their decay products are compared with the corresponding experimental α half-lives [1]. The calculations are done for zero angular momentum transfers.

Parent nuclei	Q_α(expt.) MeV	T_{SF} (s)	$T^{\alpha}_{1/2}$					Mode of decay
			Expt.	CPPM	CPPMDN	VSS	Royer [67]	
$^{294}118$	11.81 ± 0.06	3.048×10^{8}	$0.69^{+0.64}_{-0.22}$ ms	$2.58^{-0.75}_{+1.06}$ ms	$0.53^{-0.16}_{+0.22}$ ms	$0.64^{-0.18}_{+0.24}$ ms	$0.39^{-0.11}_{+0.14}$ ms	$\alpha 1$
^{290}Lv	11.00 ± 0.08	6.392×10^{3}	$8.3^{+3.5}_{-1.9}$ ms	$73.6^{-28.8}_{+48.1}$ ms	$20.8^{-8.2}_{+13.8}$ ms	$15.2^{-5.7}_{+9.0}$ ms	$8.94^{-3.31}_{+5.33}$ ms	$\alpha 2$
^{286}Fl	10.33 ± 0.06	2.372×10^{0}	$0.12^{+0.04}_{-0.02}$ s	$1.19^{-0.40}_{+0.59}$ s	$0.17^{-0.06}_{+0.09}$ s	$0.21^{-0.06}_{+0.10}$ s	$0.12^{-0.04}_{+0.06}$ s	$\alpha 3$
^{282}Cn	≤ 10.69	8.200×10^{-4}[a]	—	23.51 ms	4.89 ms	5.71 ms	3.29 ms	SF

[a]Experimental SF half-life taken from Ref. [1].

Stable nuclei usually occur in a very narrow band in the Z-N plane close to the $Z = N$ line and all other nuclei decay spontaneously in various ways and are hence unstable. Most of the SHN lie far away from the $Z = N$ line and hence are highly unstable, with very short half-lives. The existence of stable nuclei implies to the fact that the overall net nucleon-nucleon force must be attractive and much stronger than the Coulomb force; otherwise, the nuclei would collapse in on themselves. In heavier nuclei, the binding energy is found to be smaller because of the larger Coulomb repulsion and for still heavier masses, nuclei can decay spontaneously into two or more lighter nuclei, provided the mass of the parent nucleus is larger than the sum of the masses of the daughter nuclei. As the superheavy isotopes synthesized in various fusion reactions decay primarily through consecutive α emissions and get terminated by spontaneous fission, decay mechanisms like α decay, cluster decay, and spontaneous fission may be considered as the major experimental signatures for the production of SHN.

α decay, observed by Rutherford [26,27] a century ago, is one of the prominent decay modes of the SHN. As valuable information regarding the mode of decay and low-energy nuclear structure of unstable SHN can be obtained from their α decay studies, the observation and characterization of the α decay properties of the superheavy elements are very important. The production of some new SHN has resulted

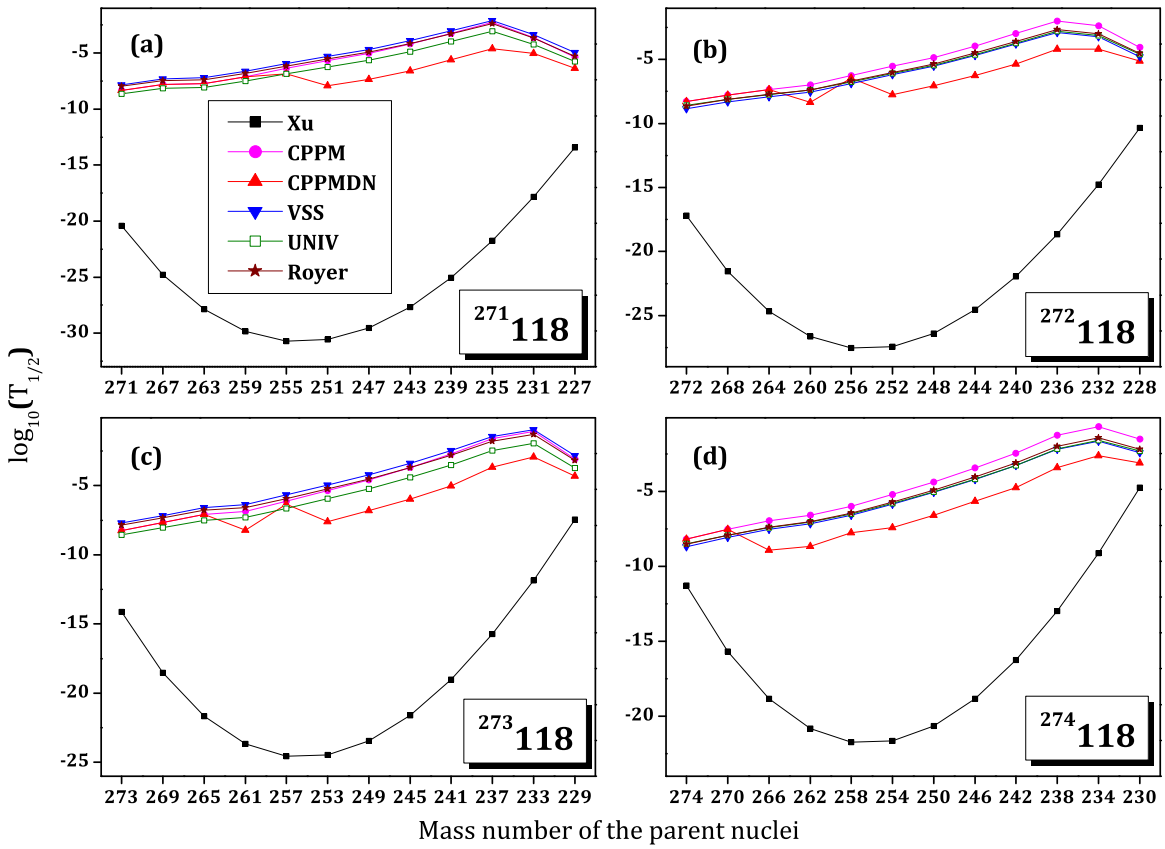

FIG. 1. (Color online) Plot for the comparison of the calculated α decay half-lives with the corresponding SF half-lives of the isotopes $^{271-274}118$ and their decay products.

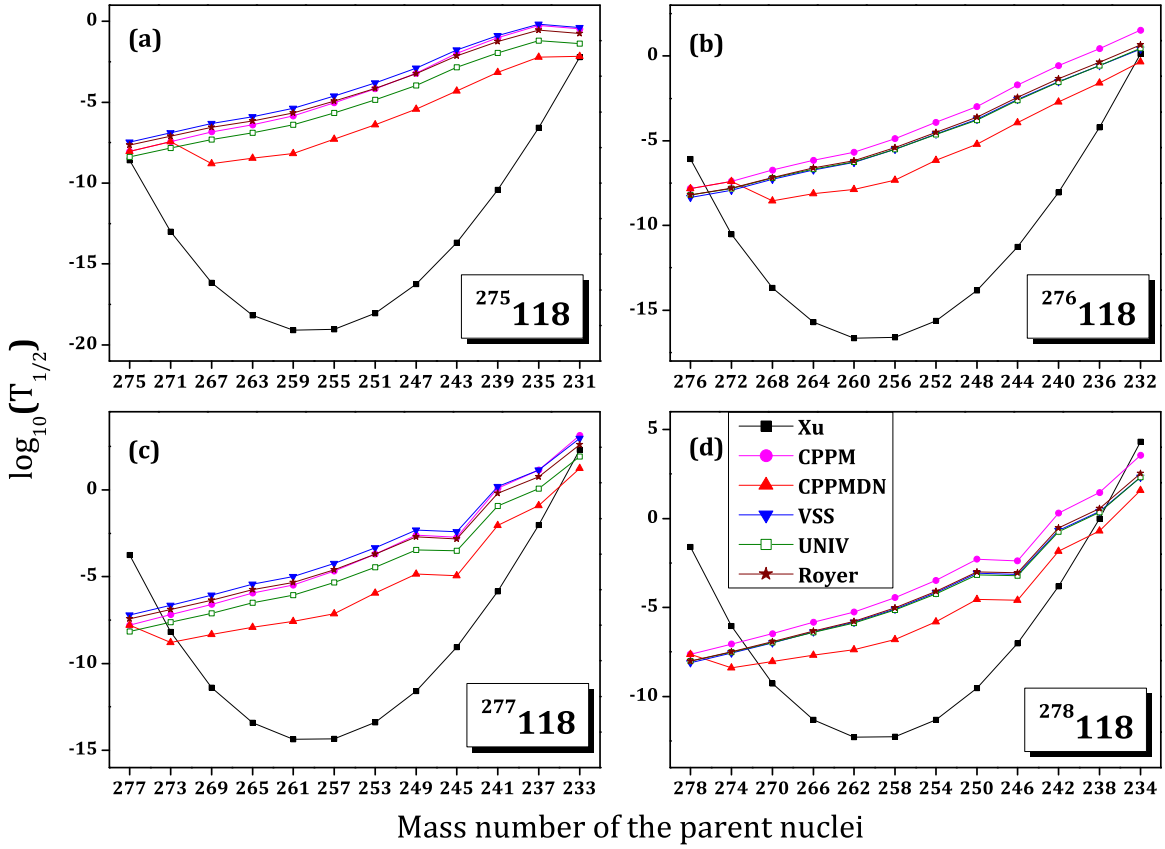

FIG. 2. (Color online) Plot for the comparison of the calculated α decay half-lives with the corresponding SF half-lives of the isotopes $^{275-278}118$ and their decay products.

in the identification of some stable α emitters in this region. The α emitters usually span an enormous range of lifetimes ranging from 10 ns to 10^{17} y and the quantum mechanical phenomenon of tunneling may be attributed to the origin of this large spread. The theoretical and experimental studies on the superheavy elements may result in many new findings, especially the possible appearance of new magic shell numbers or more precisely the prediction of the doubly magic nucleus next to ^{208}Pb ($Z = 82$, $N = 126$). Several theoretical models [28–33] have been employed for the predictions on the α decay of SHN and a number of theoretical studies have been performed recently [34–39], concentrating on various α decay properties of these nuclei. In the present paper, we have carried out an extensive study on the α decay of 40 isotopes of $Z = 118$, encompassing the region $271 \leqslant A \leqslant 310$, including the recently synthesized SHN ^{294}118, within the Coulomb and proximity potential model for deformed nuclei (CPPMDN) [40]. Within our formalism, we have already performed α studies on the odd-Z nuclei with $Z = 115$ [41], $Z = 117$ [42,43], and $Z = 119$ [44], thereby proving the applicability of CPPMDN in predicting the mode of decay of SHN and the present study may be considered as an extension of our earlier works to the even-Z region.

The details of the CPPMDN are presented in Sec. II, discussions on the α decay of the nuclei under study and the results obtained are given in Sec. III, and a conclusion on the entire work is given in Sec. IV.

II. THE COULOMB AND PROXIMITY POTENTIAL MODEL FOR DEFORMED NUCLEI

The potential energy barrier in CPPMDN is taken as the sum of deformed Coulomb potential, deformed two-term proximity potential, and centrifugal potential for both the touching configuration and the separated fragments. The simple power law interpolation as done by Shi and Swiatecki [45] is used for the pre-scission (overlap) region. It was observed [46] that the inclusion of the proximity potential reduces the height of the potential barrier, and this observation closely agrees with the experimental result.

Shi and Swiatecki [45] were the first to use the proximity potential in an empirical manner and, later on, several theoretical groups [47–49] used the same, quite extensively over a decade, for various studies. The contribution of both the internal and the external parts of the barrier has been considered, in the present model, for the penetrability calculation and the assault frequency, ν, is calculated for each parent-cluster combination which is associated with the vibration energy. However, for even-A parents and for odd-A parents, Shi and Swiatecki [50] get ν empirically, unrealistic values as 10^{22} and 10^{20}, respectively.

The interacting potential barrier for two spherical nuclei is given by

$$V = \frac{Z_1 Z_2 e^2}{r} + V_p(z) + \frac{\hbar^2 \ell(\ell+1)}{2\mu r^2}, \quad \text{for} \quad z > 0. \qquad (1)$$

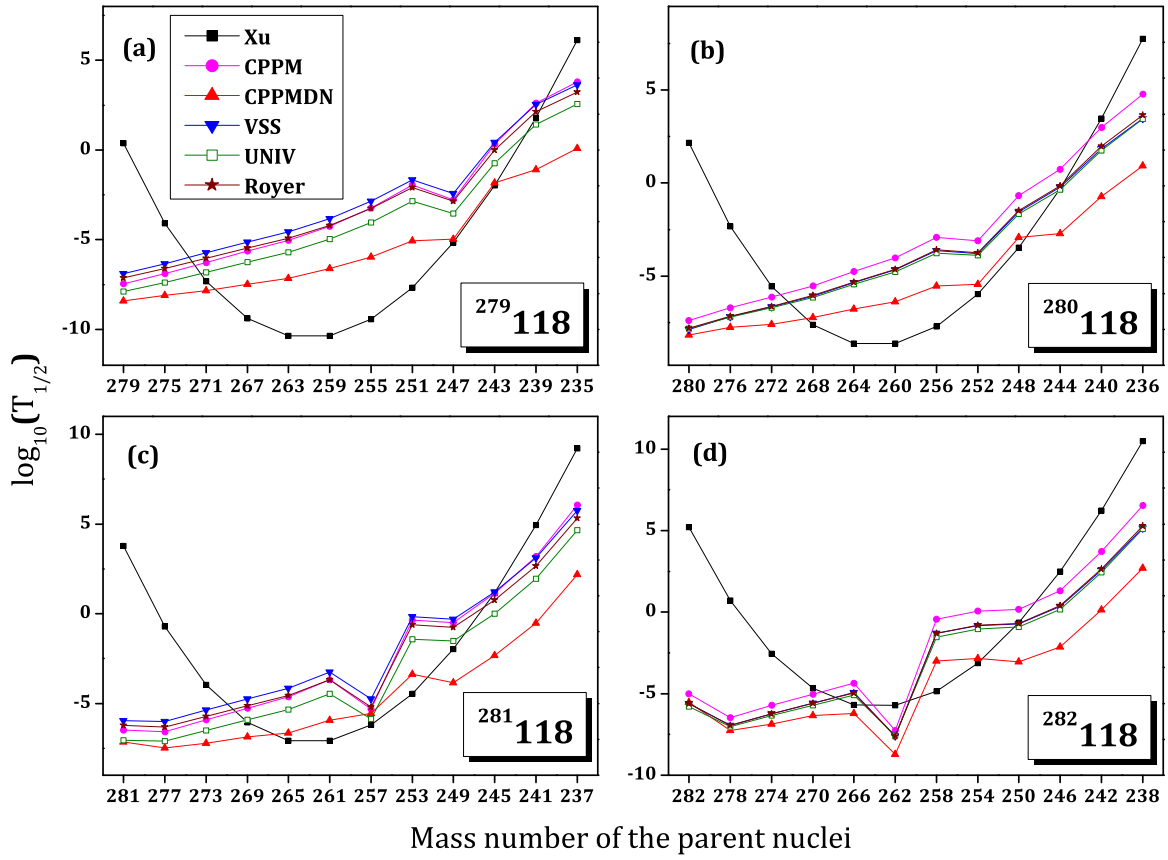

FIG. 3. (Color online) Plot for the comparison of the calculated α decay half-lives with the corresponding SF half-lives of the isotopes $^{279-282}118$ and their decay products.

Here Z_1 and Z_2 are the atomic numbers of the daughter and emitted cluster, "r" is the distance between fragment centers, "z" is the distance between the near surfaces of the fragments, ℓ represents the angular momentum, and μ the reduced mass. V_P is the proximity potential given by Blocki *et al.* [51] as

$$V_p(z) = 4\pi\gamma b\left[\frac{C_1C_2}{(C_1+C_2)}\right]\Phi\left(\frac{z}{b}\right), \tag{2}$$

with the nuclear surface tension coefficient,

$$\gamma = 0.9517[1 - 1.7826(N-Z)^2/A^2]\ \text{MeV/fm}^2. \tag{3}$$

Here N, Z, and A represent the neutron, proton, and mass number of the parent and Φ represents the universal proximity potential [52] given as

$$\Phi(\varepsilon) = -4.41e^{-\varepsilon/0.7176}, \quad \text{for} \quad \varepsilon \geqslant 1.9475, \tag{4}$$

$$\Phi(\varepsilon) = -1.7817 + 0.9270\varepsilon + 0.0169\varepsilon^2 - 0.05148\varepsilon^3, \quad \text{for} \quad 0 \leqslant \varepsilon \leqslant 1.9475, \tag{5}$$

with $\varepsilon = z/b$, where the width (diffuseness) of the nuclear surface $b \approx 1$ and the Süsmann central radii C_i of the fragments is related to the sharp radii R_i as

$$C_i = R_i - \left(\frac{b^2}{R_i}\right). \tag{6}$$

For R_i, we use a semiempirical formula in terms of mass number A_i as [51]

$$R_i = 1.28A_i^{1/3} - 0.76 + 0.8A_i^{-1/3}. \tag{7}$$

The potential for the internal part (overlap region) of the barrier is given as

$$V = a_0(L - L_0)^n, \quad \text{for} \quad z < 0, \tag{8}$$

where $L = z + 2C_1 + 2C_2$ and $L_0 = 2C$, the diameter of the parent nuclei. The constants a_0 and n are determined by the smooth matching of the two potentials at the touching point.

Using the one-dimensional WKB approximation, the barrier penetrability P is given as

$$P = \exp\left\{-\frac{2}{\hbar}\int_a^b \sqrt{2\mu(V-Q)}dz\right\}. \tag{9}$$

Here the mass parameter is replaced with $\mu = mA_1A_2/A$, where m is the nucleon mass and A_1, A_2 are the mass numbers of daughter and emitted clusters, respectively. The turning points "a" and "b" are determined from the equation, $V(a) = V(b) = Q$. The above integral can be evaluated numerically or analytically, and the half-life time is given by

$$T_{1/2} = \left(\frac{\ln 2}{\lambda}\right) = \left(\frac{\ln 2}{\upsilon P}\right), \tag{10}$$

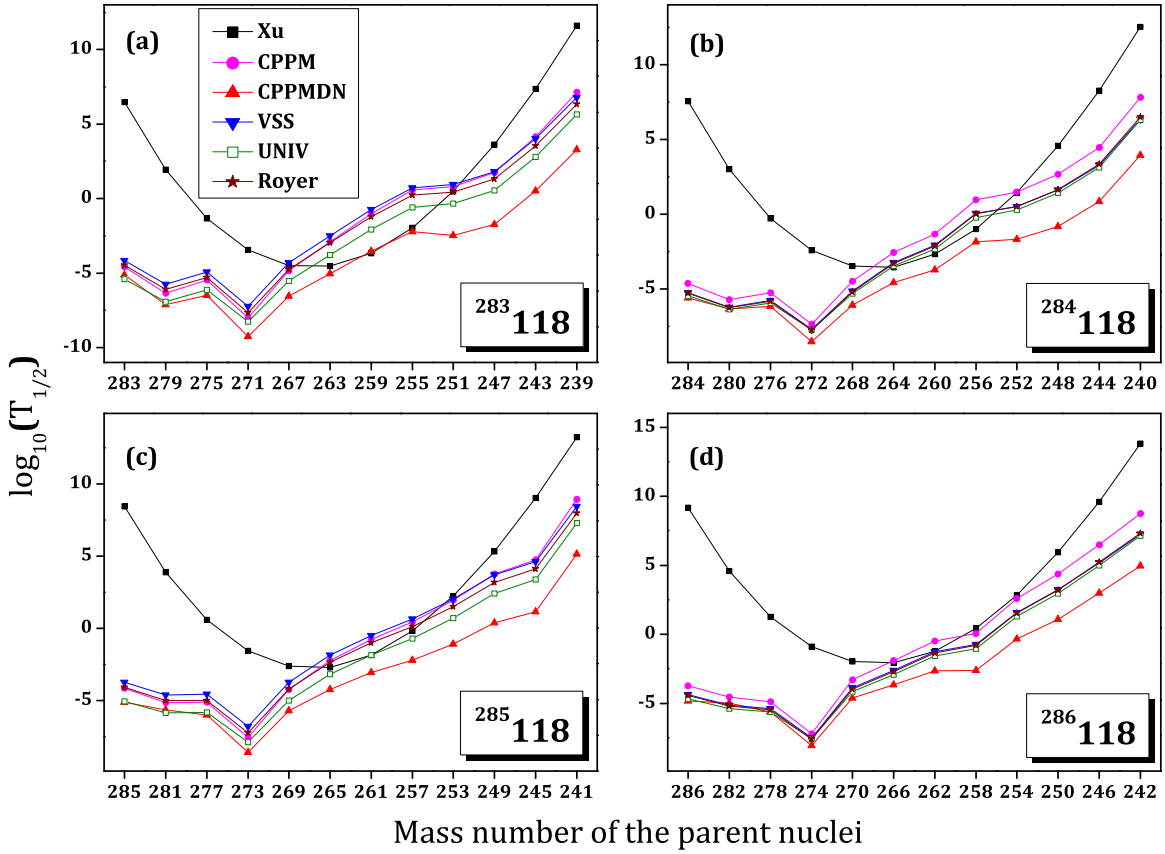

FIG. 4. (Color online) Plot for the comparison of the calculated α decay half-lives with the corresponding SF half-lives of the isotopes $^{283-286}118$ and their decay products.

where $\nu = (\frac{\omega}{2\pi}) = (\frac{2E_v}{h})$ represent the number of assaults on the barrier per second and λ the decay constant. E_v, the empirical vibration energy, is given as [53]

$$E_v = Q\left\{0.056 + 0.039\exp\left[\frac{(4-A_2)}{2.5}\right]\right\}, \quad \text{for} \quad A_2 \geqslant 4 \tag{11}$$

Classically, the α particle is assumed to move back and forth in the nucleus and the usual way of determining the assault frequency is through the expression given by $\nu =$ velocity$/(2R)$, where R is the radius of the parent nuclei. However, as the α particle has wave properties, a quantum mechanical treatment is more accurate. Thus, assuming that the α particle vibrates in a harmonic oscillator potential with a frequency ω, which depends on the vibration energy E_v, we can identify this frequency as the assault frequency ν given in Eqs. (10) and (11).

The Coulomb interaction between the two deformed and oriented nuclei with higher multipole deformation included [54,55] is taken from Ref. [56] and is given as

$$V_C = \frac{Z_1 Z_2 e^2}{r} + 3Z_1 Z_2 e^2 \sum_{\lambda,i=1,2} \frac{1}{2\lambda+1}\frac{R_{0i}^{\lambda}}{r^{\lambda+1}} Y_{\lambda}^{(0)}(\alpha_i) \times\left[\beta_{\lambda i} + \frac{4}{7}\beta_{\lambda i}^2 Y_{\lambda}^{(0)}(\alpha_i)\delta_{\lambda,2}\right], \tag{12}$$

with

$$R_i(\alpha_i) = R_{0i}\left[1 + \sum_{\lambda}\beta_{\lambda i} Y_{\lambda}^{(0)}(\alpha_i)\right], \tag{13}$$

where $R_{0i} = 1.28A_i^{1/3} - 0.76 + 0.8A_i^{-1/3}$. Here α_i is the angle between the radius vector and symmetry axis of the ith nuclei (see Fig. 1 of Ref. [54]) and it is to be noted that the quadrupole interaction term proportional to $\beta_{21}\beta_{22}$ is neglected because of its short range character.

The proximity potential and the double folding potential can be considered as the two variants of the nuclear interaction [57,58]. In the description of interaction between two fragments, the latter is found to be more effective. The proximity potential of Blocki *et al.* [51,52], which describes the interaction between two pure spherically symmetric fragments, has one term based on the first approximation of the folding procedure and the two-term proximity potential of Baltz *et al.* (Eq. (11) of Ref. [59]) includes the second component as the second approximation of the more accurate folding procedure. The authors have shown that the two-term proximity potential is in excellent agreement with the folding model for heavy-ion reaction, not only in shape but also in absolute magnitude (see Fig. 3 of Ref. [59]). The two-term proximity potential for interaction between a deformed and

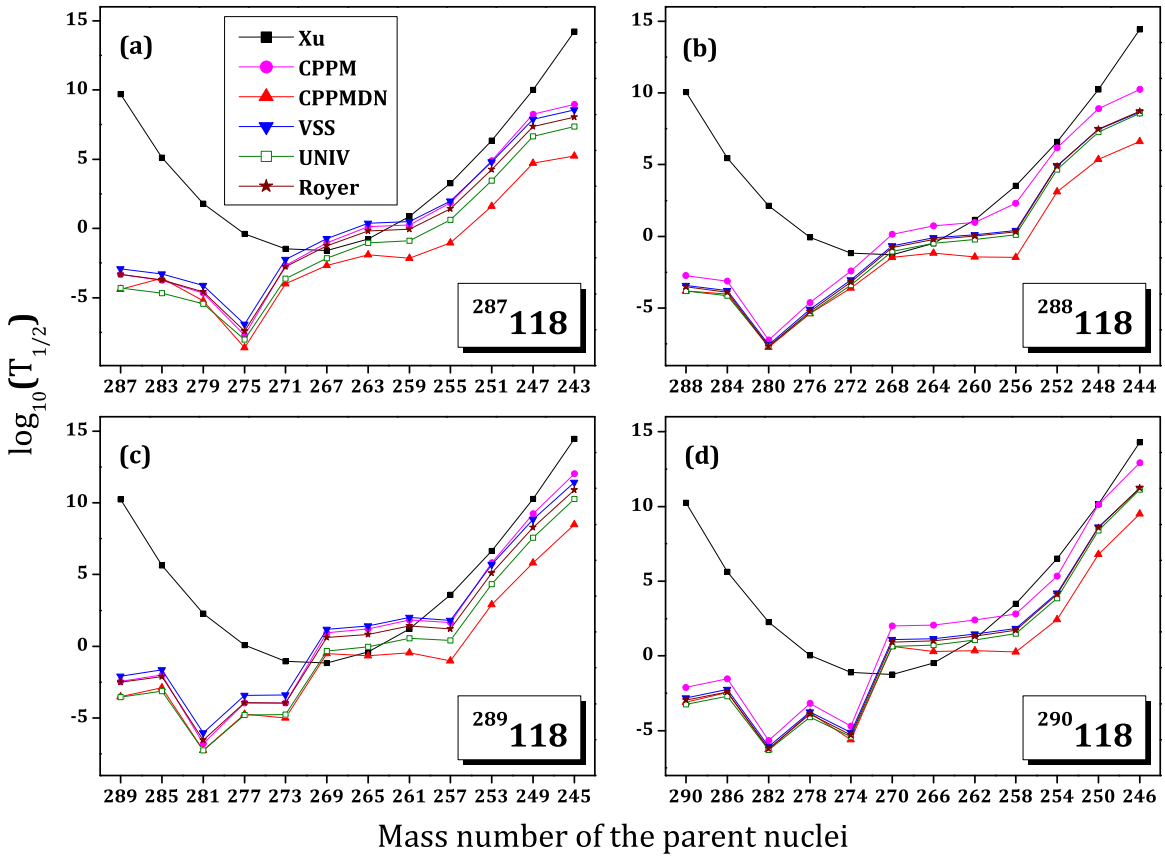

FIG. 5. (Color online) Plot for the comparison of the calculated α decay half-lives with the corresponding SF half-lives of the isotopes $^{287-290}118$ and their decay products.

spherical nucleus is given by Baltz *et al.* [59] as

$$V_{P2}(R,\theta) = 2\pi\left[\frac{R_1(\alpha)R_C}{R_1(\alpha)+R_C+S}\right]^{1/2}\left[\frac{R_2(\alpha)R_C}{R_2(\alpha)+R_C+S}\right]^{1/2} \times\left\{\left[\varepsilon_0(S)+\frac{R_1(\alpha)+R_C}{2R_1(\alpha)R_C}\varepsilon_1(S)\right] \times\left[\varepsilon_0(S)+\frac{R_2(\alpha)+R_C}{2R_2(\alpha)R_C}\varepsilon_1(S)\right]\right\}^{1/2}, \quad (14)$$

where $R_1(\alpha)$ and $R_2(\alpha)$ are the principal radii of curvature of the daughter nuclei at the point where polar angle is α, R_C is the radius of the spherical cluster, S is the distance between the surfaces along the straight line connecting the fragments, and $\varepsilon_0(S)$ and $\varepsilon_1(S)$ are the one-dimensional slab-on-slab function.

III. RESULTS AND DISCUSSIONS

The α decay half-lives of the isotopes of the SHN with $Z = 118$, within the range $271 \leqslant A \leqslant 310$, have been evaluated and studied using the CPPMDN. The external drifting potential barrier in CPPMDN is obtained as the sum of deformed Coulomb potential, deformed two-term proximity potential, and centrifugal potential. The energy released in the α transitions between the ground-state energy levels of the parent nuclei and the ground-state energy levels of the daughter nuclei, is given as

$$Q_{gs\to gs} = \Delta M_p - (\Delta M_\alpha + \Delta M_d) + k\left(Z_p^\varepsilon - Z_d^\varepsilon\right). \quad (15)$$

Here $\Delta M_p, \Delta M_d$, and ΔM_α are the mass excess of the parent, daughter, and α particle, respectively. The Q values for the α decay between the ground state of the parent and daughter nuclei have been evaluated using two different mass tables, viz., the recent experimental mass table of Wang *et al.* [60], and for those nuclei where experimental mass excess were unavailable, it was taken from Koura *et al.* [61]. As the effect of the atomic electrons on the energy of the α particle has not been included in the mass excess given in Refs. [60,61], for a more accurate calculation of Q value, the electron screening effect [62] has been included in Eq. (15). The term $k(Z_p^\varepsilon - Z_d^\varepsilon)$, where $k = 8.7$ eV and $\varepsilon = 2.517$ for nuclei with $Z \geqslant 60$ and $k = 13.6$ eV and $\varepsilon = 2.408$ for nuclei with $Z < 60$, represents this correction. For the calculation of α half-lives, the quadrupole (β_2) and hexadecapole (β_4) deformation values of both the parent and the daughter nuclei have also been used. As the experimental deformation values are not available for the nuclei considered, the theoretical values taken from Ref. [63] have been used.

A. α decay half-lives

The Viola-Seaborg semiempirical (VSS) relationship [64], the universal (UNIV) curve of Poenaru *et al.* [65,66], and the

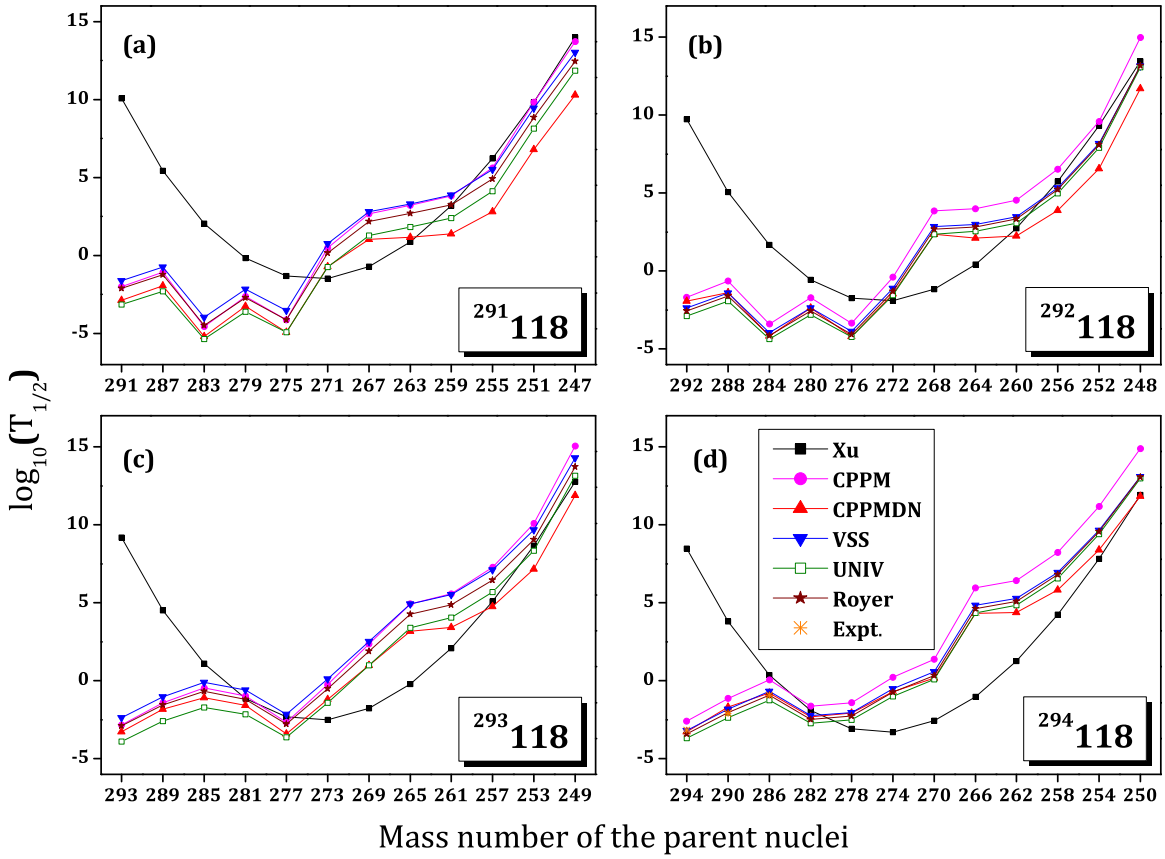

FIG. 6. (Color online) Plot for the comparison of the calculated α decay half-lives with the corresponding SF half-lives of the isotopes $^{291-294}118$ and their decay products.

analytical formulas of Royer [67] have also been used for the evaluation of the α decay half-lives of the isotopes under study. The formalisms are discussed below.

1. The Viola-Seaborg semiempirical relationship

The VSS relationship, with constants determined by Sobiczewski *et al.* [68], is given as

$$\log_{10}(T_{1/2}) = (aZ + b)Q^{-1/2} + cZ + d + h_{\log}. \quad (16)$$

Here the half-life is in seconds, the Q value is in MeV, and Z is the atomic number of the parent nucleus. The quantities a, b, c, and d are adjustable parameters and the quantity $h_{\log}$ represents the hindrances associated with odd proton and odd neutron numbers, as given by Viola and Seaborg [64]. However, instead of using the original set of constants given by Viola and Seaborg [64], more recent values determined by Sobiczewski *et al.* [68], taking account of the new data for even-even nuclei, have been used here. The constants are $a = 1.661\,75$, $b = -8.5166$, $c = -0.202\,28$, $d = -33.9069$, and

$$h_{\log} = 0, \quad \text{for } Z, N \text{ even},$$
$$h_{\log} = 0.772, \quad \text{for } Z = \text{odd}, N = \text{even},$$
$$h_{\log} = 1.066, \quad \text{for } Z = \text{even}, N = \text{odd},$$
$$h_{\log} = 1.114, \quad \text{for } Z, N \text{ odd}.$$

2. The universal curve of Poenaru et al.

The decay half-lives have been explained using several simple and effective relationships, which are obtained by fitting the experimental data. Among them, the UNIV curves [69–72], derived by extending a fission theory to larger mass asymmetry should be mentioned with great emphasis. Based on the quantum mechanical tunneling process [73,74], the disintegration constant λ, valid in both fissionlike and α-like theories, is related to the partial decay half-life T of the parent nucleus as

$$\lambda = \ln 2/T = \nu S P_S. \quad (17)$$

Here ν, S, and P_s are three model-dependent quantities: ν is the frequency of assaults on the barrier per second, S is the preformation probability of the cluster at the nuclear surface (equal to the penetrability of the internal part of the barrier in a fission theory [69,70]), and P_s is the quantum penetrability of the external potential barrier.

By using the decimal logarithm,

$$\log_{10} T(s) = -\log_{10} P - \log_{10} S + [\log_{10}(\ln 2) - \log_{10} \nu]. \quad (18)$$

To derive the universal formula, it was assumed that $\nu =$ constant and that S depends only on the mass number of the emitted particle A_e [70,73] as the microscopic calculation of the preformation probability [75] of many clusters from ^{8}Be to ^{46}Ar had shown that it is dependent only upon the size of

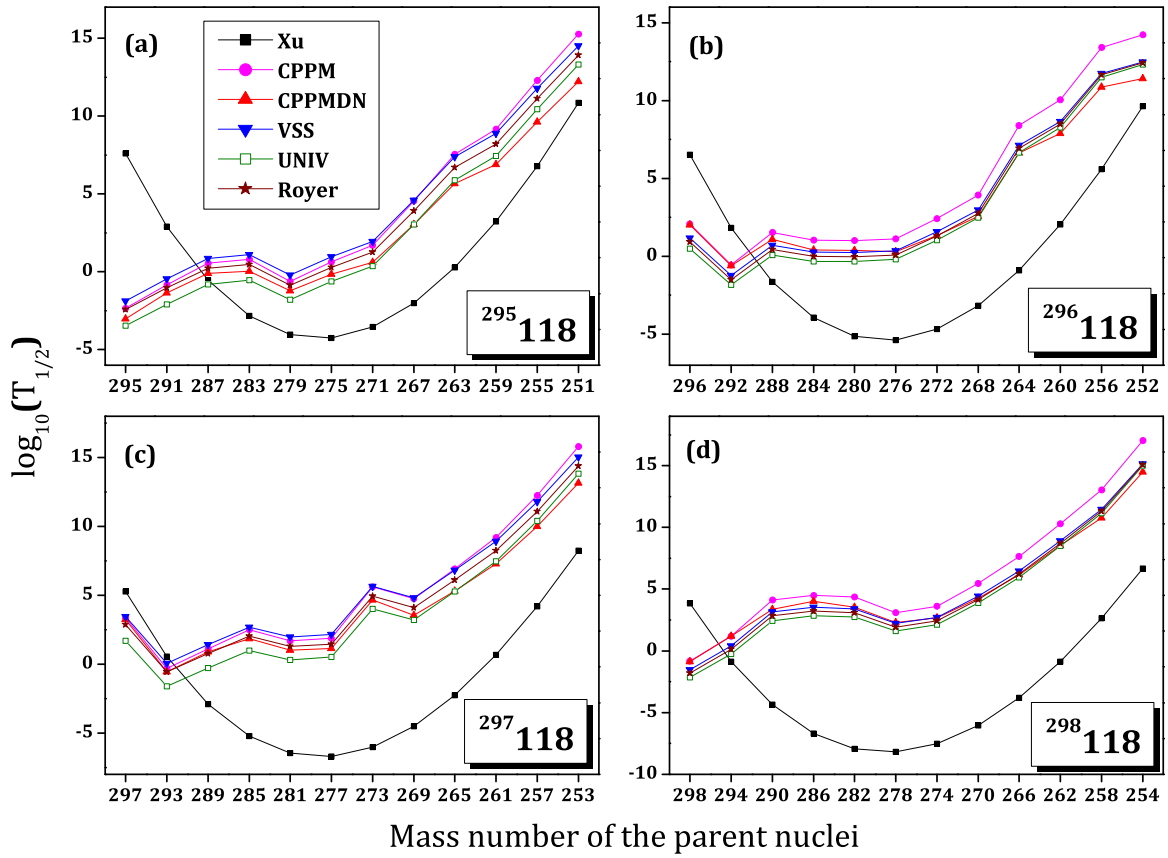

FIG. 7. (Color online) Plot for the comparison of the calculated α decay half-lives with the corresponding SF half-lives of the isotopes $^{295-298}118$ and their decay products.

the cluster. Using a fit with experimental data for α decay, the corresponding numerical values [70] obtained were $S_\alpha = 0.014\,315\,3$, $\nu = 10^{22.01}$ s^{-1}. The decimal logarithm of the preformation factor is given as

$$\log_{10} S = -0.598(A_e - 1), \tag{19}$$

and the additive constant for an even-even nucleus is

$$c_{ee} = [-\log_{10}\nu + \log_{10}(\ln 2)] = -22.16917. \tag{20}$$

The penetrability through an external Coulomb barrier, having separation distance at the touching configuration $R_a = R_t = R_d + R_e$ as the first turning point and the second turning point defined by $e^2 Z_d Z_e / R_b = Q$, may be found analytically as

$$-\log_{10} P_S = 0.228\,73(\mu_A Z_d Z_e R_b)^{1/2} \times[\arccos\sqrt{r} - \sqrt{r(1-r)}], \tag{21}$$

where $r = R_t/R_b$, $R_t = 1.2249(A_d^{1/3} + A_e^{1/3})$ and $R_b = 1.439\,98 Z_d Z_e / Q$.

The released energy Q is evaluated using the mass tables [60,61] and the liquid-drop-model radius constant $r_0 = 1.2249$ fm.

3. *The analytical formulas of Royer*

Several expressions [64,68,76,77] were developed for the α decay half-lives, subsequent to the earliest law formulated by Geiger and Nutall [78]. By applying a fitting procedure on a set of 373 α emitters, Royer [67] formulated the analytical formulas for α decay with an rms deviation of 0.42, given as

$$\log_{10}[T_{1/2}(s)] = -26.06 - 1.114A^{1/6}\sqrt{Z} + \frac{1.5837Z}{\sqrt{Q_\alpha}}. \tag{22}$$

Here A and Z are the mass and charge numbers of the parent nuclei and Q_α is the energy released during the reaction. Assuming the same dependence on the mass and charge of the mother nucleus and experimental Q_α, Eq. (22) was adjusted to a subset of 131 even-even nuclei and a relation was obtained with a rms deviation of only 0.285 and is given as

$$\log_{10}[T_{1/2}(s)] = -25.31 - 1.169A^{1/6}\sqrt{Z} + \frac{1.5864Z}{\sqrt{Q_\alpha}}. \tag{23}$$

For a subset of 106 even-odd nuclei the rms deviation was found to be 0.39, and the relation is given as

$$\log_{10}[T_{1/2}(s)] = -26.65 - 1.0859A^{1/6}\sqrt{Z} + \frac{1.5848Z}{\sqrt{Q_\alpha}}. \tag{24}$$

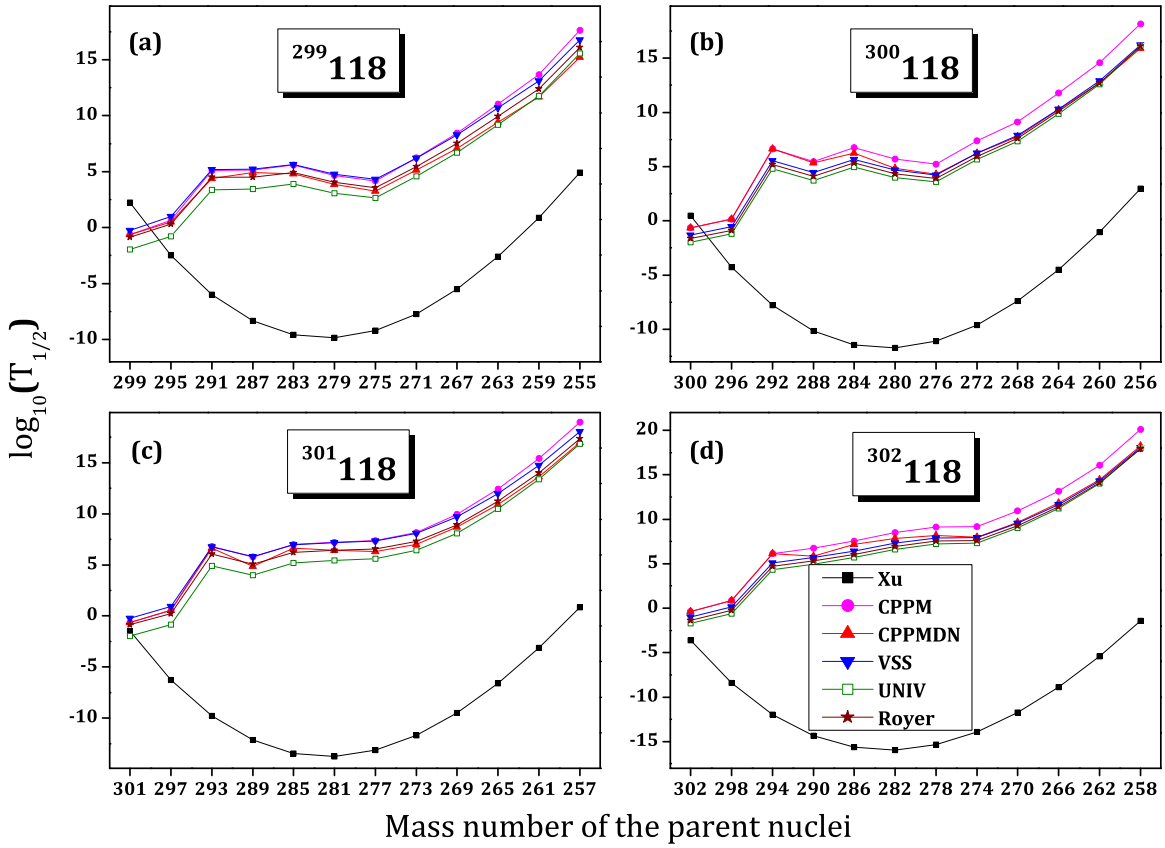

FIG. 8. (Color online) Plot for the comparison of the calculated α decay half-lives with the corresponding SF half-lives of the isotopes $^{299-302}118$ and their decay products.

B. Spontaneous-fission half-lives

The mode of decay of the isotopes under study can be identified through the calculations on the spontaneous-fission (SF) half-lives of the corresponding nuclei. The semiempirical relation given by Xu *et al.* [79], originally made to fit the even-even nuclei, has been used for evaluating the SF half-lives and is given as

$$T_{1/2} = \exp\left\{2\pi\left[C_0 + C_1 A + C_2 Z^2 + C_3 Z^4 + C_4 (N-Z)^2 - \left(0.133\,23\frac{Z^2}{A^{1/3}} - 11.64\right)\right]\right\}. \quad (25)$$

Here the constants $C_0 = -195.092\,27$, $C_1 = 3.101\,56$, $C_2 = -0.043\,86$, $C_3 = 1.4030 \times 10^{-6}$, and $C_4 = -0.031\,99$.

Attempts to synthesize the superheavy element with Z = 118 has been under progress since 1999 [2], and recently Oganessian *et al.* [1,2] have been successful in the synthesis of the $^{294}118$ isotope and have determined the α decay properties of $^{294}118$ and its successive decay products. Hence, in the present study, the α decay properties of $^{294}118$ isotope have been studied separately and are given in Table I. The isotope under study and the corresponding decay products in the α decay chain are given in the first column, and in column 2 the respective experimental Q values available are shown. The experimental α decay half-lives taken from Ref. [1] are given in column 4. The experimental Q values have been used for the evaluation of the α half-lives and the calculations done within both our formalisms, the Coulomb and proximity potential model (CPPM) and the CPPMDN [including the ground-state quadrupole (β_2) and hexadecapole (β_4) deformation of both the parent and the daughter nuclei], are given in the columns 5 and 6, respectively. On comparison of the experimental half-lives with the half-lives evaluated using CPPMDN, it can be seen that the calculated values are in good agreement with the experimental values. The α half-lives evaluated using the semiempirical VSS formula and the analytical formulas of Royer have been given in columns 7 and 8, respectively. The mode of decay of the isotopes is shown in column 9. In column 3 of the Table I, we have shown the SF half-lives of the corresponding isotopes, evaluated using the phenomenological formula of Xu *et al.* [79]. As the isotopes with smaller α decay half-lives than the SF half-lives survive fission and could be detected through α decay in the laboratory, a comparison of the α half-lives with the corresponding SF half-lives leads us to predict the mode of decay and thereby identify the nuclei (both parent and decay products) that will survive fission. Thus, through such a comparison, we have predicted 3α chains from $^{294}118$ and it is noteworthy that our predictions go hand in hand with the observation of Oganessian *et al.* [1,2].

As we could successfully reproduce the experimental data for $^{294}118$ using our formalism, we have confidently extended our study to predict the α half-lives and the mode of decay

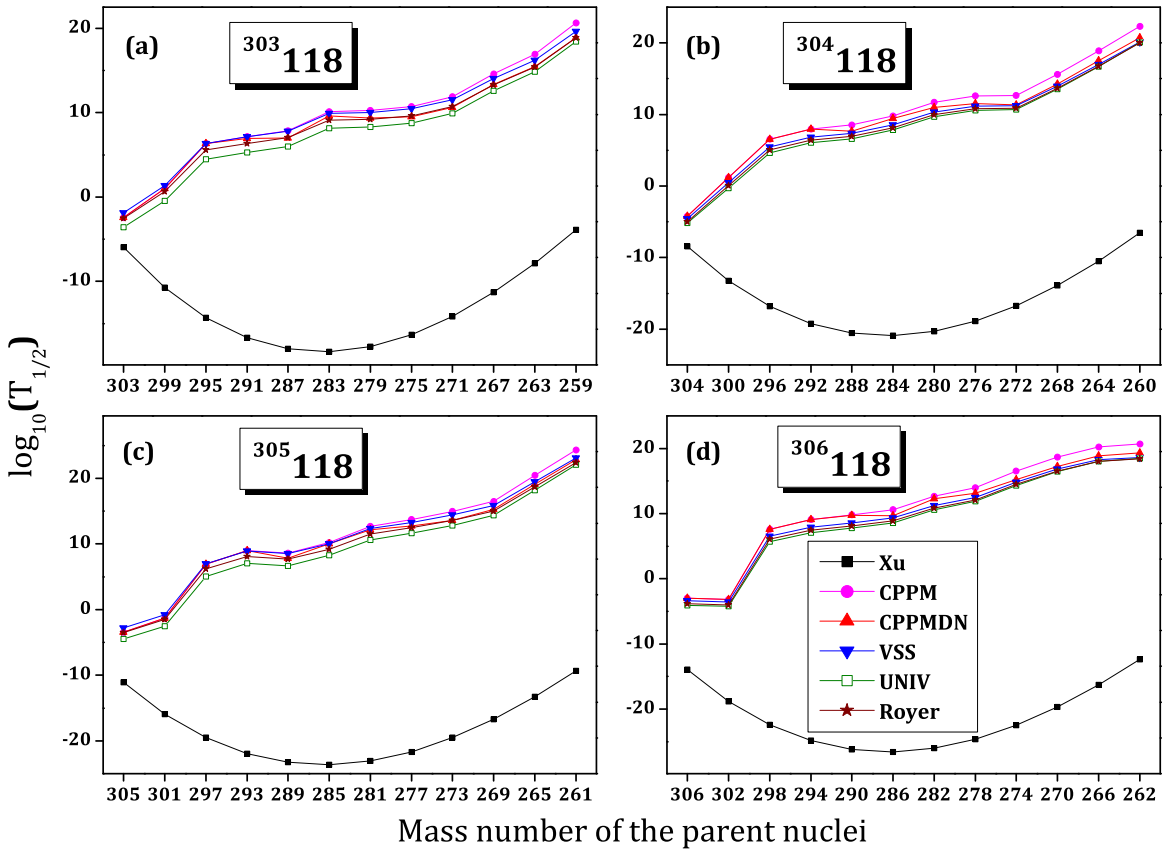

FIG. 9. (Color online) Plot for the comparison of the calculated α decay half-lives with the corresponding SF half-lives of the isotopes $^{303-306}118$ and their decay products.

of the isotopes of $Z = 118$ ranging from $271 \leqslant A \leqslant 310$. The entire work is presented in Figs. 1–10, where we have plotted the $\log_{10}(T_{1/2})$ against the mass number of the parent nuclei in the corresponding α chain. The plots for the decay half-lives calculated using both CPPM and CPPMDN have been shown in these figures and it can be seen that the α half-lives decrease when the deformation values are included. Along with these, we have plotted the decay half-lives evaluated using the VSS formula; the UNIV and the analytical formulas of Royer for comparison and these values agree well with our theoretical calculations. The SF half-lives computed using the phenomenological formula of Xu *et al.* are also given in these figures. The evaluated SF half-lives have been compared with the experimental SF half-lives [80] and were found to be in agreement with each other. For example, in the case of ^{253}Rf, $T_{\rm sf}^{\rm expt.} = 4.800 \times 10^{-5}$ s and $T_{\rm sf}^{\rm calc.} = 3.451 \times 10^{-5}$ s; and in the case of ^{250}Cm, $T_{\rm sf}^{\rm expt.} = 3.537 \times 10^{11}$ s and $T_{\rm sf}^{\rm calc.} = 8.109 \times 10^{11}$ s, which shows the agreement between the experimental and the evaluated SF half-lives.

Figure 1 represents the plot of $\log_{10}(T_{1/2})$ versus mass number for the nuclei $^{271-274}118$. A comparison of α half-life with the corresponding SF half-life makes it clear that none of these isotopes survive fission. The plots for the nuclei $^{275-278}118$ and $^{279-282}118$ are given in Figs. 2 and 3, respectively. It can be seen that, except for the $^{275}118$ isotope, all these nuclei survive fission and 1α chain can be observed from $^{276}118$, 2α from $^{277,278}118$, 3α from $^{279,280}118$, 4α from $^{281}118$, and 6α from $^{282}118$. Figures 4 and 5 represent the plot for $^{283-286}118$ and $^{287-290}118$, respectively. These figures clearly depict that all these isotopes survive fission and 6α chains can be observed from $^{283}118$. However, it can be seen from these figures that the α half-lives, evaluated using CPPMDN, of both the parent and the daughter isotopes of $Z = 118$ in the range $284 \leqslant A \leqslant 288$ are much below the millisecond region (for e.g., $T_{1/2}^{\alpha} = 2.650 \times 10^{-6}$ s for $^{284}118$, $T_{1/2}^{\alpha} = 7.444 \times 10^{-6}$ s for $^{285}118$ and for $^{274}112$, $T_{1/2}^{\alpha} = 8.609 \times 10^{-9}$ s) and their decay chain do not end with SF. Hence, these isotopes cannot be predicted to be detectable in laboratories, through α decay. The isotopes $^{289}118$ and $^{290}118$ shown in Figs. 5(c) and 5(d) survive fission and 5α chains can be observed from these isotopes. The plot of $\log_{10}(T_{1/2})$ versus mass number for the nuclei $^{291-294}118$ and $^{295-298}118$, which includes the experimentally synthesized nuclei $^{294}118$, is shown in Figs. 6 and 7, respectively. As seen, 5α chains can be observed from $^{291-293}118$ and thus these isotopes survive fission. The Fig. 6(d) gives the calculations done for the experimentally synthesized nuclei $^{294}118$ and as the experimental Q values were available for the nuclei and its decay products, we have used these Q values for the calculation of the α decay half-lives and have already presented in the Table I. In the case of $^{294}118$, as the experimental Q values were available only up to the decay product $^{282}112$, in Fig. 6(d), we have plotted the α decay half-lives that were calculated using the experimental Q values up to the decay product $^{282}112$. The α decay half-lives for

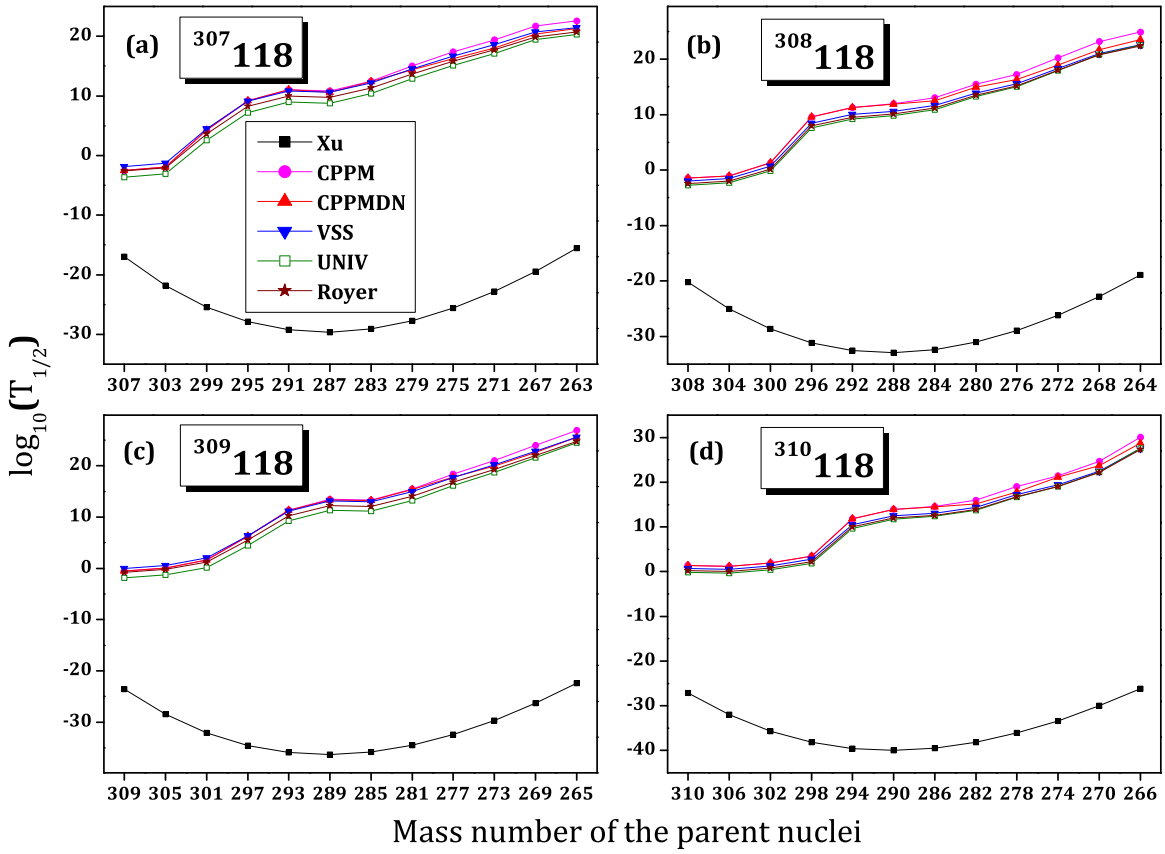

FIG. 10. (Color online) Plot for the comparison of the calculated α decay half-lives with the corresponding SF half-lives of the isotopes $^{307-310}118$ and their decay products.

the remaining decay products have been evaluated using the Q values that were calculated using the mass excess values taken from Refs. [60,61]. A comparison of the T_{sf} values calculated using the semiempirical relation given by Xu *et al.*, and the α decay half-lives predicts 3α chains for $^{294}118$, which closely agrees with the experimentally observed facts [1,2]. The experimental α decay values have been represented as scattered points in this figure. Also from our calculations we have predicted two α chains from the nuclei $^{295-297}118$ and one α chain to be seen from the isotope $^{298}118$.

As we could observe 5α chains consistently from the nuclei $^{289-293}118$, we have predicted that these nuclei could

TABLE II. Comparison of the α half-lives and SF half-lives of $^{289,290}118$ and their decay products. A prediction on the mode of decay is given by comparing the α decay half-lives with the SF half-lives. The calculations are done for zero angular momentum transfers.

Parent nuclei	Q_α(cal) MeV	T_{SF} (s)	$T^{\alpha}_{1/2}$(s)					Mode of decay
			CPPM	CPPMDN	VSS	UNIV	Royer [67]	
$^{289}118$	11.785	1.776×10^{10}	3.614×10^{-3}	3.055×10^{-4}	8.478×10^{-3}	2.833×10^{-4}	3.116×10^{-3}	α1
^{285}Lv	11.355	4.357×10^{5}	1.021×10^{-2}	1.311×10^{-3}	2.352×10^{-2}	7.673×10^{-4}	7.993×10^{-3}	α2
^{281}Fl	13.165	1.894×10^{2}	1.655×10^{-7}	5.575×10^{-8}	9.174×10^{-7}	5.493×10^{-8}	2.951×10^{-7}	α3
^{277}Cn	11.625	1.195×10^{0}	1.111×10^{-4}	1.920×10^{-5}	3.912×10^{-4}	1.644×10^{-5}	1.168×10^{-4}	α4
^{273}Ds	11.365	9.016×10^{-2}	1.096×10^{-4}	9.909×10^{-6}	4.014×10^{-4}	1.749×10^{-5}	1.130×10^{-4}	α5
^{269}Hs	9.365	6.707×10^{-2}	9.131×10^{0}	3.011×10^{-1}	1.497×10^{1}	4.795×10^{-1}	4.051×10^{0}	SF
$^{290}118$	11.645	1.792×10^{10}	7.817×10^{-3}	8.213×10^{-4}	1.548×10^{-3}	5.601×10^{-4}	1.112×10^{-3}	α1
^{286}Lv	11.175	4.263×10^{5}	2.909×10^{-2}	3.711×10^{-3}	5.548×10^{-3}	1.945×10^{-3}	3.887×10^{-3}	α2
^{282}Fl	12.625	1.795×10^{2}	2.221×10^{-6}	5.391×10^{-7}	8.949×10^{-7}	5.077×10^{-7}	6.197×10^{-7}	α3
^{278}Cn	11.305	1.098×10^{0}	6.607×10^{-4}	1.533×10^{-4}	1.813×10^{-4}	7.871×10^{-5}	1.239×10^{-4}	α4
^{274}Ds	11.665	8.017×10^{-2}	1.990×10^{-5}	2.518×10^{-6}	7.388×10^{-6}	3.913×10^{-6}	5.006×10^{-6}	α5
^{270}Hs	9.045	5.776×10^{-2}	9.952×10^{1}	4.371×10^{0}	1.227×10^{1}	4.217×10^{0}	8.583×10^{0}	SF
^{266}Sg	8.805	3.398×10^{-1}	1.124×10^{2}	1.986×10^{0}	1.389×10^{1}	5.143×10^{0}	9.931×10^{0}	SF

TABLE III. Comparison of the α half-lives and SF half-lives of $^{291-293}118$ and their decay products. A prediction on the mode of decay is given by comparing the α decay half-lives with the SF half-lives. The calculations are done for zero angular momentum transfers.

Parent nuclei	Q_α(cal) MeV	T_{SF} (s)	$T^{\alpha}_{1/2}$(s)					Mode of decay
			CPPM	CPPMDN	VSS	UNIV	Royer [67]	
$^{291}118$	11.595	1.199×10^{10}	1.008×10^{-2}	1.305×10^{-3}	2.367×10^{-2}	7.000×10^{-4}	8.001×10^{-3}	$\alpha 1$
^{287}Lv	10.995	2.764×10^{5}	8.511×10^{-2}	1.104×10^{-2}	1.817×10^{-1}	5.061×10^{-3}	5.671×10^{-2}	$\alpha 2$
^{283}Fl	12.135	1.128×10^{2}	2.702×10^{-5}	6.419×10^{-6}	1.085×10^{-4}	4.415×10^{-6}	3.199×10^{-5}	$\alpha 3$
^{279}Cn	11.085	6.679×10^{-1}	2.326×10^{-3}	5.677×10^{-4}	7.016×10^{-3}	2.387×10^{-4}	1.929×10^{-3}	$\alpha 4$
^{275}Ds	11.425	4.725×10^{-2}	7.244×10^{-5}	1.204×10^{-5}	2.935×10^{-4}	1.206×10^{-5}	7.617×10^{-5}	$\alpha 5$
^{271}Hs	9.505	3.297×10^{-2}	3.042×10^{0}	1.880×10^{-1}	5.785×10^{0}	1.751×10^{-1}	1.441×10^{0}	SF
^{267}Sg	8.625	1.878×10^{-1}	4.629×10^{2}	1.072×10^{1}	6.240×10^{2}	1.874×10^{1}	1.514×10^{2}	SF
$^{292}118$	11.465	5.319×10^{9}	2.096×10^{-2}	1.161×10^{-2}	4.165×10^{-3}	1.339×10^{-3}	2.739×10^{-3}	$\alpha 1$
^{288}Lv	10.835	1.188×10^{5}	2.251×10^{-1}	4.056×10^{-2}	4.001×10^{-2}	1.206×10^{-2}	2.566×10^{-2}	$\alpha 2$
^{284}Fl	11.645	4.696×10^{1}	3.833×10^{-4}	6.826×10^{-5}	1.125×10^{-4}	4.490×10^{-5}	7.130×10^{-5}	$\alpha 3$
^{280}Cn	10.735	2.694×10^{-1}	1.907×10^{-2}	4.365×10^{-3}	4.392×10^{-3}	1.546×10^{-3}	2.756×10^{-3}	$\alpha 4$
^{276}Ds	11.105	1.846×10^{-2}	4.383×10^{-4}	6.203×10^{-5}	1.378×10^{-4}	5.851×10^{-5}	8.593×10^{-5}	$\alpha 5$
^{272}Hs	9.785	1.247×10^{-2}	4.039×10^{-1}	3.486×10^{-2}	7.892×10^{-2}	2.805×10^{-2}	5.004×10^{-2}	SF
^{268}Sg	8.295	6.880×10^{-2}	7.214×10^{3}	2.221×10^{2}	7.137×10^{2}	2.336×10^{2}	4.733×10^{2}	SF
$^{293}118$	11.915	1.564×10^{9}	1.475×10^{-3}	5.267×10^{-4}	4.260×10^{-3}	1.270×10^{-4}	1.337×10^{-3}	$\alpha 1$
^{289}Lv	11.105	3.384×10^{4}	3.983×10^{-2}	1.516×10^{-2}	9.628×10^{-2}	2.550×10^{-3}	2.777×10^{-2}	$\alpha 2$
^{285}Fl	10.515	1.296×10^{1}	3.605×10^{-1}	8.117×10^{-2}	7.819×10^{-1}	1.984×10^{-2}	2.100×10^{-1}	$\alpha 3$
^{281}Cn	10.465	7.205×10^{-2}	1.029×10^{-1}	2.601×10^{-2}	2.532×10^{-1}	6.957×10^{-3}	6.409×10^{-2}	$\alpha 4$
^{277}Ds	10.835	4.782×10^{-3}	2.116×10^{-3}	3.846×10^{-4}	7.126×10^{-3}	2.346×10^{-4}	1.707×10^{-3}	$\alpha 5$
^{273}Hs	9.725	3.129×10^{-3}	5.913×10^{-1}	6.499×10^{-2}	1.354×10^{0}	3.936×10^{-2}	3.104×10^{-1}	SF
^{269}Sg	8.705	1.671×10^{-2}	2.244×10^{2}	1.002×10^{1}	3.407×10^{2}	9.535×10^{0}	7.611×10^{1}	SF

be synthesized and detected experimentally via α decay. However, even though we could observe consistent 3α, 4α, and 6α chains from $^{279,280}118$, $^{281}118$, and $^{282,283}118$, respectively, these nuclei could not be predicted to be synthesized in the laboratories as their decay half-lives are too small, which span the order 10^{-9} to 10^{-6} s. Most of the predicted, unknown nuclei in the range $289 \leqslant A \leqslant 293$ were found to have relatively long half-lives and hence could be sufficient to detect them if synthesized in a laboratory. These predictions are highlighted in Tables II and III as we hope this observation provides a new guide to the experiments progressing on $Z = 118$. In the tables, the Q_α values represent the difference in the mass excess of the parent and the fragments.

The plots for the nuclei $^{299-302}118$, $^{303-306}118$, and $^{307-310}118$ are given in Figs. 8, 9, and 10 respectively. Of these nuclei, $^{299-300}118$ isotopes survive fission and give one α chain, whereas the nuclei $^{301-310}118$ are found to undergo SF completely and thus will not survive fission. Hence, our calculations on the heavy mass isotopes of $Z = 118$ punctuates the fact, as no isotope below $A \leqslant 275$ and above $A \geqslant 301$ survives fission, the α decay is restricted within the range $276 \leqslant A \leqslant 300$.

Recently, within the dinuclear system model with dynamical potential energy surface (DNS-DyPES model), Wang *et al.* [81], have studied the excitation functions for producing SHN with $Z = 118$ in some ^{48}Ca-induced reactions and the possibilities for producing the same element with other entrance channels at different mass asymmetries such as ^{50}Ti + ^{248}Cm and ^{54}Cr + ^{244}Pu were also investigated. The authors have evaluated and predicted the excitation functions for ^{48}Ca + $^{250-252}$Cf and the dependence of the evaporation residue (ER) cross sections for producing the residue nuclei $^{293-297}118$. Their study revealed that the maximum effective ER cross sections for the productions of $^{294}118$, $^{295}118$, and $^{296}118$ were about 0.2-0.5 pb, close to the current experimental limit, and that for $^{293}118$ and $^{297}118$ were about 0.1 pb. It can be seen that the study aims at making predictions for the experiment being under way at the FLNR of JINR in Dubna, Russia, and the predictions highlight the isotopes $^{293-297}118$. In the present work, as we have predicted 5α, 3α, and 2α chains consistently from the nuclei $^{289-293}118$, $^{294}118$, and $^{295-297}118$ respectively, which includes the isotopes highlighted by Wang *et al.*, we hope that our studies will also accelerate the experiments in progress at JINR, FLNR, Dubna.

We would also like to place emphasis on the fact that the present work, whereby a comparison of the α decay half-lives and SF half-lives predicts the mode of decay of a vast range of isotopes, is the first theoretical work done on the α decay properties of $Z = 118$.

IV. CONCLUSION

The feasibility of α decay from the isotopes of the SHN with $Z = 118$, which span the range $271 \leq A \leqslant 310$, has been studied extensively by taking the external drifting potential barrier as the sum of deformed Coulomb potential, deformed two-term proximity potential, and centrifugal potential (within CPPMDN). The formalism could be considered

unimpeachable as we were successful in reproducing the experimental α half-lives and the decay chains observed for $^{294}118$. We thus confidently counted in 39 more isotopes of $Z = 118$ with an aim of predicting the α decay chains of all the isotopes in this region. Through our study, we have lightened the fact that those isotopes of $Z = 118$ with $A \geqslant 301$ and with $A \leqslant 275$ do not survive fission and thus the α decay is retrenched to the range $276 \leqslant A \leqslant 300$. We anticipate that our predictions of 5α chains consistently from $^{289-293}118$, 3α chains from $^{294}118$, and 2α chains from $^{295-297}118$ would accelerate the experiments in progress for the synthesis of new isotopes of $Z = 118$.

ACKNOWLEDGMENTS

K.P.S. would like to thank the University Grants Commission, Government of India, for the financial support under Major Research Project. No. 42-760/2013 (SR) dated 22-03-2013.

[1] Yu. Ts. Oganessian *et al.*, Phys. Rev. Lett. **109**, 162501 (2012).
[2] Yu. Ts. Oganessian *et al.*, Phys. Rev. C **74**, 044602 (2006).
[3] M. A. Stoyer, Nature (London) **442**, 876 (2006).
[4] Yu. Ts. Oganessian *et al.*, Phys. Rev. C **72**, 034611 (2005).
[5] Yu. Ts. Oganessian *et al.*, Phys. Rev. C **62**, 041604(R) (2000).
[6] Yu. Ts. Oganessian *et al.*, Eur. Phys. J. A **15**, 201 (2002).
[7] Yu. Ts. Oganessian *et al.*, Nucl. Phys. A **734**, 109 (2004).
[8] S. Hofmann and G. Münzenberg, Rev. Mod. Phys. **72**, 733 (2000).
[9] Yu. Ts. Oganessian, J. Phys. G: Nucl. Part. Phys. **34**, R165 (2007).
[10] Yu. Ts. Oganessian, Nucl. Phys. A **685**, 17c (2001).
[11] P. Armbruster, Annu. Rev .Nucl. Part. Sci. **35**, 135 (1985).
[12] P. Armbruster, Annu. Rev. Nucl. Part. Sci. **50**, 411 (2000).
[13] G. Münzenberg, S. Hofmann, F. P. Heßberger, W. Reisdorf, K. H. Schmidt, J. H. R. Schneider, P. Armbruster, C. C. Sahm, and B. Thuma, Z. Phys. A **300**, 107 (1981).
[14] Yu. Ts. Oganessian *et al.*, Phys. Rev. Lett. **104**, 142502 (2010).
[15] Yu. Ts. Oganessian *et al.*, Phys. Rev. C **83**, 054315 (2011).
[16] Yu. Ts. Oganessian, A. S. Iljinov, A. G. Demin, and S. P. Tretyakova, Nucl. Phys. A **239**, 353 (1975).
[17] G. Münzenberg, P. Armbruster, F. P. Heßberger, S. Hofmann, K. Poppensieker, W. Reisdorf, J. H. R. Schneider, W. F. W. Schneider, K. H. Schmidt, C. C. Sahm, and D. Vermeulen, Z. Phys. A **309**, 89 (1982).
[18] D. Ackermann, Nucl. Phys. A **787**, 353c (2007).
[19] S. Hofmann, D. Ackermann, S. Antalic, H. G. Burkhard, V. F. Comas, R. Dressler, Z. Gan, S. Heinz, J. A. Heredia, and F. P. Heßberger, Eur. Phys. J. A **32**, 251 (2007).
[20] S. Hofmann, F. P. Heßberger, D. Ackermann, S. Antalic, P. Cagarda, B. Kindler, P. Kuusiniemi, M. Leino, B. Lommel, O. N. Malyshev, R. Mann, G. Münzenberg, A. G. Popeko, S. Saro, B. Streicher, and A. V. Yeremin, Nucl. Phys. A **734**, 93 (2004).
[21] S. Hofmann, G. Munzenberg, and M. Schadel, Nucl. Phys. News **14**, 5 (2004).
[22] K. Morita, K. Morimoto, D. Kaji, T. Akiyama, S. Goto, H. Haba, E. Ideguchi, K. Katori, H. Koura, H. Kikunaga, H. Kudo, T. Ohnishi, A. Ozawa, N. Sato, T. Suda, K. Sueki, F. Tokanai, T. Yamaguchi, A. Yoneda, and A. Yoshida, J. Phys. Soc. Jpn. **76**, 045001 (2007).
[23] K. Morita, K. Morimoto, D. Kaji, T. Akiyama, S. Goto, H. Haba, E. Ideguchi, R. Kanungo, K. Katori, H. Koura, H. Kudo, T. Ohnishi, A. Ozawa, T. Suda, K. Sueki, H. S. Xu, T. Yamaguchi, A. Yoneda, A. Yoshida, and Y. L. Zhao, J. Phys. Soc. Jpn. **73**, 2593 (2004).
[24] K. Morita *et al.*, Nucl. Phys. A **734**, 101 (2004).
[25] K. Morita, K. Morimoto, D. Kaji, T. Akiyama, Sin-ichi Goto, H. Haba, E. Ideguchi, K. Katori, H. Koura, H. Kudo, T. Ohnishi, A. Ozawa, T. Suda, K. Sueki, F. Tokanai, T. Yamaguchi, A. Yoneda, and A. Yoshida, J. Phys. Soc. Jpn. **76**, 043201 (2007).
[26] E. Rutherford and H. Geiger, Proc. R. Soc. London, Ser. A **81**, 162 (1908).
[27] E. Rutherford and T. Royds, Phil. Mag. **17**, 281 (1909).
[28] P. Moller and J. R. Nix, Nucl. Phys. A **549**, 84 (1992).
[29] H. F. Zhang and G. Royer, Phys. Rev. C **76**, 047304 (2007).
[30] P. R. Chowdhury, D. N. Basu, and C. Samanta, Phys. Rev. C **75**, 047306 (2007).
[31] D. S. Delion, R. J. Liotta, and R. Wyss, Phys. Rev. C **76**, 044301 (2007).
[32] Z. Ren and C. Xu, J. Phys.: Conf. Ser. **111**, 012040 (2008).
[33] V. Yu. Denisov and A. A. Khudenko, At. Data Nucl. Data Tables **95**, 815 (2009).
[34] A. I. Budaca and I. Silişteanu, Phys. Rev. C **88**, 044618 (2013).
[35] Y. Qian, Z. Ren, and D. Ni, Phys. Rev. C **89**, 024318 (2014).
[36] P. Jachimowicz, M. Kowal, and J. Skalski, Phys. Rev. C **89**, 024304 (2014).
[37] Niyti and R. K. Gupta, Phys. Rev. C **89**, 014603 (2014).
[38] Y. J. Liang, M. Zhu, Z. H. Liu, and W. Z. Wang, Phys. Rev. C **89**, 034627 (2014).
[39] L. Zhu, W. J. Xie, and F. S. Zhang, Phys. Rev. C **89**, 024615 (2014).
[40] K. P. Santhosh, S. Sabina, and G. J. Jayesh, Nucl. Phys. A **850**, 34 (2011).
[41] K. P. Santhosh, B. Priyanka, G. J. Jayesh, and S. Sahadevan, Phys. Rev. C **84**, 024609 (2011).
[42] K. P. Santhosh, B. Priyanka, and M. S. Unnikrishnan, Phys. Rev. C **85**, 034604 (2012).
[43] K. P. Santhosh and B. Priyanka, J. Phys. G: Nucl. Part. Phys. **39**, 085106 (2012).
[44] K. P. Santhosh and B. Priyanka, Phys. Rev. C **87**, 064611 (2013).
[45] Y. J. Shi and W. J. Swiatecki, Nucl. Phys. A **438**, 450 (1985).
[46] K. P. Santhosh and A. Joseph, Pramana J. Phys. **62**, 957 (2004).
[47] S. S. Malik, S. Singh, R. K. Puri, S. Kumar, and R. K. Gupta, Pramana J. Phys. **32**, 419 (1989).
[48] I. Dutt and R. K. Puri, Phys. Rev. C **81**, 064608 (2010).
[49] I. Dutt and R. K. Puri, Phys. Rev. C **81**, 064609 (2010).
[50] Y. J. Shi and W. J. Swiatecki, Nucl. Phys. A **464**, 205 (1987).
[51] J. Blocki, J. Randrup, W. J. Swiatecki, and C. F. Tsang, Ann. Phys. (NY) **105**, 427 (1977).
[52] J. Blocki and W. J. Swiatecki, Ann. Phys. (NY) **132**, 53 (1981).
[53] D. N. Poenaru, M. Ivascu, A. Sandulescu, and W. Greiner, Phys. Rev. C **32**, 572 (1985).

[54] N. Malhotra and R. K. Gupta, Phys. Rev. C **31**, 1179 (1985).
[55] R. K. Gupta, M. Balasubramaniam, R. Kumar, N. Singh, M. Manhas, and W. Greiner, J. Phys. G: Nucl. Part. Phys. **31**, 631 (2005).
[56] C. Y. Wong, Phys. Rev. Lett. **31**, 766 (1973).
[57] N. V. Antonenko and R. V. Jolos, Z. Phys. A **339**, 453 (1991).
[58] N. V. Antonenko, E. A. Cherepanov, A. K. Nasirov, V. P. Permjakov, and V. V. Volkov, Phys. Rev. C **51**, 2635 (1995).
[59] A. J. Baltz and B. F. Bayman, Phys. Rev. C **26**, 1969 (1982).
[60] M. Wang, G. Audi, A. H. Wapstra, F. G. Kondev, M. MacCormick, X. Xu, and B. Pfeiffer, Chin. Phys. C **36**, 1603 (2012).
[61] H. Koura, T. Tachibana, M. Uno, and M. Yamada, Prog. Theor. Phys. **113**, 305 (2005).
[62] V. Y. Denisov and H. Ikezoe, Phys. Rev. C **72**, 064613 (2005).
[63] P. Möller, J. R. Nix, and K. L. Kratz, At. Data Nucl. Data Tables **66**, 131 (1997).
[64] V. E. Viola, Jr., and G. T. Seaborg, J. Inorg. Nucl. Chem. **28**, 741 (1966).
[65] D. N. Poenaru, R. A. Gherghescu, and W. Greiner, Phys. Rev. C **83**, 014601 (2011).
[66] D. N. Poenaru, R. A. Gherghescu, and W. Greiner, Phys. Rev. C **85**, 034615 (2012).
[67] G. Royer, J. Phys. G: Nucl. Part. Phys. **26**, 1149 (2000).
[68] A. Sobiczewski, Z. Patyk, and S. Cwiok, Phys. Lett. B **224**, 1 (1989).
[69] D. N. Poenaru and W. Greiner, J. Phys. G: Nucl. Part. Phys. **17**, S443 (1991).
[70] D. N. Poenaru and W. Greiner, Phys. Scr. **44**, 427 (1991).
[71] D. N. Poenaru, I. H. Plonski, and W. Greiner, Phys. Rev. C **74**, 014312 (2006).
[72] D. N. Poenaru, I. H. Plonski, R. A. Gherghescu, and W. Greiner, J. Phys. G: Nucl. Part. Phys. **32**, 1223 (2006).
[73] R. Blendowske and H. Walliser, Phys. Rev. Lett. **61**, 1930 (1988).
[74] R. Blendowske, T. Fliessbach, and H. Walliser, in *Nuclear Decay Modes* (Institute of Physics Publishing, Bristol, 1996), Chap. 7, p. 337.
[75] M. Iriondo, D. Jerrestam, and R. J. Liotta, Nucl. Phys. A **454**, 252 (1986).
[76] Z. Patyk, A. Sobiczewski, P. Armbruster, and K. H. Schmidt, Nucl. Phys. A **491**, 267 (1989).
[77] B. A. Brown, Phys. Rev. C **46**, 811 (1992).
[78] H. Geiger and J. M. Nutall, Phil. Mag. **22**, 613 (1911).
[79] C. Xu, Z. Ren, and Y. Guo, Phys. Rev. C **78**, 044329 (2008).
[80] National Nuclear Data Centre, NuDat2.5, http://www.nndc.bnl.gov.
[81] N. Wang, E. G. Zhao, and W. Scheid, Phys. Rev. C **89**, 037601 (2014).